

LASER BIOLOGY

PACS numbers: 87.64. – t; 42.62.Be; 42.87. – d
DOI: 10.1070/QE2006v036n09ABEH013408

Peculiarities of studying an isolated neuron by the method of laser interference microscopy

A.I. Yusipovich, S.M. Novikov, T.A. Kazakova, L.A. Erokhova, N.A. Brazhe, G.L. Lazarev, G.V. Maksimov

***Abstract*. Actual aspects of using a new method of laser interference microscopy (LIM) for studying nerve cells are discussed. The peculiarities of the LIM display of neurons are demonstrated by the example of isolated neurons of a pond snail *Lymnaea stagnalis*. A comparative analysis of the images of the cell and subcellular structures of a neuron obtained by the methods of interference microscopy, optical transmission microscopy, and confocal microscopy is performed. Various aspects of the application of LIM for studying the lateral dimensions and internal structure of the cytoplasm and organelles of a neuron in cytology and cell physiology are discussed.**

Keywords: *laser interference microscopy, neuron, cytoplasm.*

1. Introduction

Modern laser interferometry is widely used for studying the dynamics of the shape and cellular structure of biological objects [1 – 7]. It is also applied in technology to determine the structure of the surface relief of materials, providing high-resolution measurements of the individual morphology of the relief [8, 9]. The imaging of biological objects with the help of biological microscopes based on profilometers in which low-power lasers are used as a radiation source is based on a change in the optical density of a biological object, which can be measured quantitatively [1 – 3, 5 – 7, 10 – 12]. At present laser interference microscopy (LIM) is used in biology to estimate variations of an individual cell (variations in its volume and shape) and subcellular organelles (variations in the volume, shape, and motion of subcellular organelles and actomyosin complexes of a cytoplasm) [1, 3, 5 – 7, 10 – 12]. However, it is obvious that the possibilities of this method are not realised in the study of functioning nerve cells. The specific feature of this object is a very strong dependence of the functional state and cellular dynamics on the investigation method. Probe fluorescence and confocal microscopy, as well as the microelectrode technique can initiate numerous artefacts studied in cells. We studied earlier by the LIM method dynamics variations in the optical density of the plasma membrane of a myelin nerve fibre upon generation and rhythmic excitation and of an isolated neuron during the action of neurotransmitters [1, 2, 4, 10, 11].

In this paper, we analysed in detail the possibility of using LIM for studying the cellular dynamics of a functioning neuron and obtaining the 'phase' image of a whole cell and its subcellular structure (cytoplasmic granules).

A.I. Yusipovich, T.A. Kazakova, L.A. Erokhova, N.A. Brazhe, G.V. Maksimov Department of Biology, M.V. Lomonosov Moscow State University, Vorob'evy gory, 119992 Moscow, Russia;
e-mail: maxim@biophys.msu.ru;
S.M. Novikov Department of Physics, M.V. Lomonosov Moscow State University, Vorob'evy gory, 119992 Moscow, Russia;
e-mail: serj@tls.msk.ru;
G.L. Lazarev Amphora Laboratories Limited Liability Company, Presnenskii val 17b, office 701, 123557 Moscow, Russia;
e-mail: grisha@amphoralabs.ru

Received 9 December 2005; revision received 17 May 2006
Kvantovaya Elektronika **36** (9) 874 – 878 (2006)
Translated by M.N. Sapozhnikov

2. Laser interference microscopy

It is known that LIM is used for studying the distribution of variations in the phase of the optical density of an object. The LIM method is based on the measurement of local phases of a light wave reflected by the object [13]. The interference pattern of the object is obtained due to the overlap of the reflected wave and the wave reflected from a reference mirror. Then, the signal is normalised over the wavelength, thereby determining the path difference for the two waves or the phase height (thickness) Φ of the object at the given point:

$$\Phi = \frac{\varphi_0 - \varphi_{\rm obj}}{2\pi}\frac{\lambda}{2} - \Phi_0, \qquad (1)$$

where φ_0 is the initial phase (rad); $\varphi_{\rm obj}$ is the phase shift (rad) caused by the object; λ is the radiation wavelength (nm); Φ_0 is a constant phase shift determined by the choice of the initial point of phase reference (nm).

Thus, the phase portrait of a cell is the distribution of the phase shift in different regions of the object; the obtained phase shifts are used to construct the volume (three-dimensional) image of the cell.

Biological objects (isolated nerve cells) were studied on a mirror substrate reflecting the light propagated through a cell. As a result, the double phase shift of a coherent light beam was detected at each point of the cell and the interference image of the cell was produced with the help of the additional wave from the same radiation source. In other words, reflection from different parts of the mirror substrate on which a semitransparent biological object was

localised was recorded by the LIM method. The distribution of the optical density of the biological object [the phase distribution of the wave reflected from the object ('phase height')] is found from the expression

$$\Phi(x,y) = \int_0^{z_{\max}} [n(x,y,z) - n_1]\mathrm{d}z - \Phi_0, \quad (2)$$

where n_1 is the refractive index of the buffer solution whose value is constant; $n(x,y,z)$ is the refractive index at a point of the cell with coordinates x, y and height z; and $z_{\max}$ is the upper limit of integration.

It is obvious that the total phase image of a whole cell (the cell area multiplied by the phase height of the object) contains contributions of variations in the cell volume and shape and in the refractive index of the plasma membrane, subcellular structures, and cytoplasm. Therefore, the phase height at a given point is a sum of the heights z_i of different optical media at this point multiplied by the corresponding refractive indices n_i^m minus the corresponding product of the refractive index and height of the buffer solution:

$$\Phi = \left(n_1^m z_1 + n_2^m z_2 + \ldots + n_n^m z_n\right) - n_1 z. \quad (3)$$

It is obvious that the relationship between optical media with different refractive indices (plasma membrane, molecular cytoplasm complexes, nucleus, mitochondria, chloroplast, etc.) at each point of a cell is different. The total change in the optical density at a point is independent of the sequence at which a beam propagates through different media. Therefore, even if the refractive index is known for each subcellular structure, it is rather difficult to estimate in the general case the real height of an object at the given point from its phase height. Thus, because the term 'phase height' adopted for the description of a change in the optical density of biological objects [1, 2, 4–7, 10–12, 14] does not reflect the real situation and can be used only to estimate the given parameter at each point of the biological object, it is more correct to speak about the width of the object at each point. A disadvantage of LIM is that this method does not allow the reconstruction of the three-dimensional relief of biological objects. This method can be used, however, to detect quantitatively a change in the optical density, which in the case of homogeneous objects with the known refractive index, for example, erythrocytes gives the estimate of their volume.

Biological objects are colourless and semitransparent and have a small size and low-contrast. To study their structure and functions by optical microscopy, it is necessary to increase their contrast. As a rule, this causes the modification of biological objects, for example, after their staining with dyes. Dyes used for staining not only improve the resolution of the method but change the functional state of a biological object (for example, fluorescence probes stimulate photoinduced damage of cells). The use of phase-contrast methods considerably improves the contrast of biological cells without their additional modification, which gives more correct information on processes proceeding in cells. The LIM method not only increases the contrast of samples but also makes it possible to estimate quantitatively a change in the optical density, thereby providing not only qualitative but also quantitative information on variations in the state of cells.

It is obvious that the resolution of LIM substantially determines the scope of biological objects that can be studied by this method. At present various modifications of this method are used for high-resolution investigations of the phase profiles of various nonbiological objects. It was shown that the resolution in the study of homogeneous objects with a high reflectance was better than 0.5 nm along the vertical and 10–100 nm along the horizontal, i.e. much higher than the classical resolution limit of optical microscopes [8, 9, 15]. However, in the case of weakly reflecting samples, the reflection of a beam from the surface is low, which impairs the resolution of the device, and the resolution begins to depend on the properties of the object itself. Nevertheless, the resolution of LIM in the study of biological objects is not worse that the resolution of optical microscopes, which is determined by the Rayleigh criterion [16]

$$D = \frac{0.61\lambda}{\mathrm{NA}}, \quad (4)$$

where D is the coefficient of lateral expansion between two points; λ is the laser wavelength; and NA is the numerical aperture of the objective. It is rather difficult to estimate in practice how much the resolution of images of biological objects obtained by LIM is better that the resolution obtained with optical microscopes because it depends on the properties of the object itself and can vary in each particular case.

Biological objects are studied by using, as a rule, lasers emitting in the range between 450 and 700 nm (red lasers are applied more often because cells are damaged by their radiation to a lesser degree than by radiation from blue and green lasers). Thus, if a 480-nm laser and an immersion objective with the NA = 1.4 is used in the LIM method, the horizontal resolution is no more than 200 nm. In this case, the depth of focus T of the image in LIM is defined as for optical microscopes [16]:

$$T = \frac{n\lambda}{(\mathrm{NA})^2}, \quad (5)$$

where n is the refractive index of the immersion ($n = 1$ for dry objectives).

Therefore, the depth of focus for LIM with a 480-nm laser and the objective NA = 1.4 is about 250 nm. If the objective with a high aperture is used, the horizontal resolution is increased but the depth of focus is decreased, and it becomes difficult to obtain the volume image of an object with a comparatively large variation in the optical density. When the phase height of an object exceeds the depth of focus, the recording of variations in the phase height is accompanied by jumps caused by transitions to the next interference fringe. When the angle of incidence of light is smaller than 30°, the reconstruction of the real profile of the optical relief exceeding $\lambda/2$ is possible but time consuming and does not provide the full recovery of the volume image of the object.

The LIM method can be used for studying plant and animal cells as well as bacteria and some separated organelles, for example, mitochondria (Fig. 1). These objects can be also studied by other microscopic methods, however, LIM offers the following advantages:

(i) Unmodified biological objects can be investigated in the functional state;

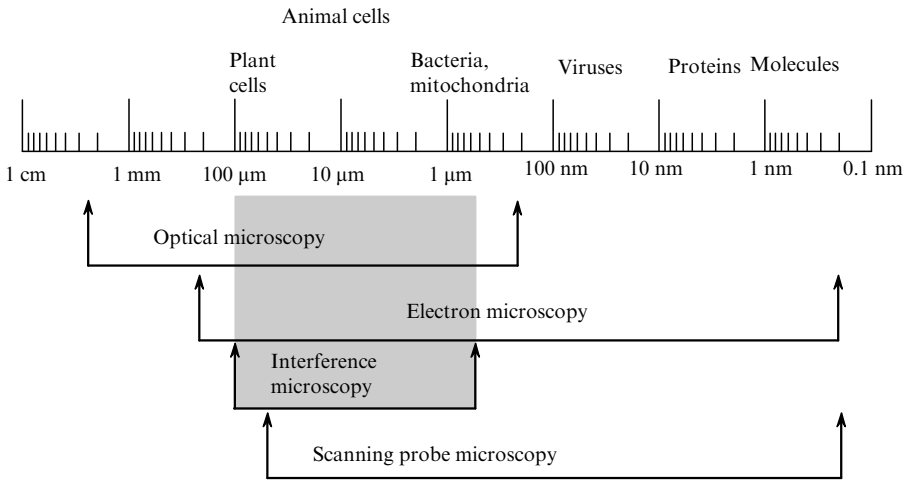

Figure 1. Fields of application of various microscopy methods in the study of biological objects.

(ii) the distribution of the phase height (thickness) of a cell and its organelles can be estimated under native, functional conditions; the volume image of the object can be obtained and its real dimensions can be estimated;

(iii) the resolution of laser interference microscopes is better than that of conventional optical microscopes;

(iv) variations in the optical density of the object at each point characterise not only the external relief of the object but also the state of the cytoplasm and its organelles [see expressions (2) and (3)];

(v) the study of the dynamics of local variations in the optical density in different regions of a cell makes it possible to observe regular variations in the optical density of a cellular structure and to estimate the frequency of regular processes in the cell and its organelles [4, 8–10].

3. Experimental

The phase images of nerve cells were obtained by using a MIM-2.1 microscope (Amphora, Russia) based on a modified Linnik microinterferometer with separated optical paths of the object and reference arms, a laser mirror being used as the reference object. In the reference arm of the microscope, which was identical to the object arm, a mirror was mounted on a piezoelectric element which performed a regular motion thereby providing the intensity modulation of the interference pattern on a photodetector. The phase of the interference pattern was recorded by the method of 'time intervals' in each element of the photodetector, which increased the measurement accuracy compared to other methods. By analysing variations in the interference pattern intensity at each point, the phase shift caused by variations in the optical parameters of the object was determined. The results of measurements were presented as the distribution of the phase shifts of radiation reflected from the object in the image plane. The object was illuminated by a normally incident quasi-plane wave.

Phase shifts were analysed by using the MIMsoft® software package which provided the estimate of the phase shift with an accuracy of 0.01 nm. The influence of external factors was reduced by using both a mechanical system and the optical channel for compensating instabilities of the setup. The radiation source in a MIM-2.1 microscope was a thermally stabilised single-mode highly coherent (the coherence length was more than 10 m) 532-nm, 40-mW laser (radiation power incident on the object was 2 mW) [8, 9, 15]. A $27^{\times}$ objective with the NA = 0.15 was used in experiments. The results were processed by using expression (1).

We studied isolated neurons of a pond snail *Lymnae stagnalis*. Cells of diameter 20–50 μm were selected for investigation. Isolated neurons were placed on a reflecting substrate (aluminium mirror covered with Al_2O_3) filled with solution containing 50 mM of NaCl, 1.5 mM of KCl, 4 mM of $CaCl_2$, 1 mM of $MgCl_2$, and 11 mM of HEPES at pH 7.5. The refractive index of the solution at the D line measured with an IRF-454 BM refractometer at temperature 18–22 °C was 1.335. The neuron image obtained by the LIM method was compared with the imaged obtained with an Axioscope FS2mot confocal microscope equipped with an LSM 510* system (Zeiss, Germany). The fluorescence of cells was excited by an argon laser at 488 nm and detected at 505 nm. An Achroplam $40^{\times}$ objective with the NA = 0.8 and confocal aperture 108 μm was used. As a rule, the 2D images of a neuron were obtained after four repeated scans along each of the lines and processing by using the Zeiss LSM Image Browser program.

4. Results and discussion

Figure 2 shows the typical phase image of a pond snail neuron. Note that the lateral dimensions of neurons obtained by LIM and other methods coincide, as a rule.

Consider the features of LIM mapping of biological objects in more detail. As mentioned above, the phase height is the sum of phase heights z of different optical media through which a light beam propagates at the given point multiplied by the corresponding refractive indices n (3). This circumstance considerably complicates the reconstruction of the three-dimensional relief from the measured change in the optical density (phase height) of the object. The difference between the real three-dimensional relief and volume phase image is minimal upon mapping of homogeneous spherical or cylindrical cells (Fig. 3a).

The mapping of objects of a different shape involves difficulties. It is known that the subcellular structures of a cell are not homogeneous: the cytoplasm has a lower density and, hence, the lower refractive index than the membrane, nucleus or other organelles (mitochondria). In addition,

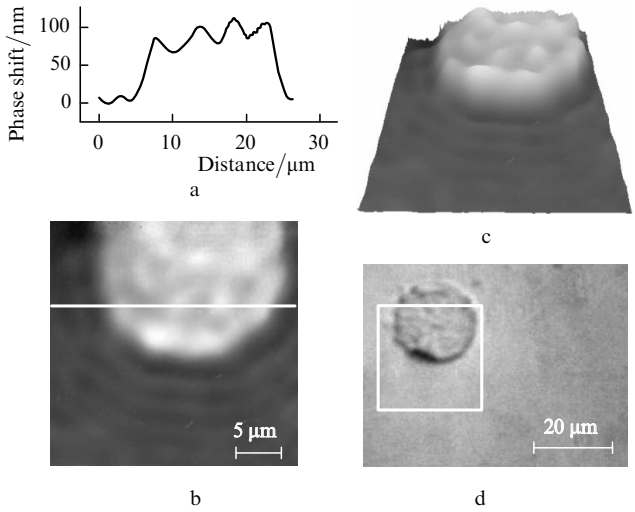

Figure 2. Isolated neuron of a pond snail *Lymnaea stagnalis*: profile of a change in the phase height (a), the phase image of a neuron (b), the volume image of a neuron (c), and the neuron image obtained with an optical microscope (d).

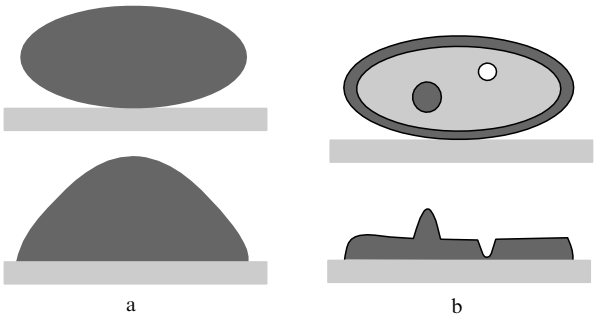

Figure 3. Cross sections of native spherical biological objects (top) with a homogeneous (a) or inhomogeneous (b) content and their phase portraits (bottom).

cellular vacuoles are filled with liquid having the refractive index that is approximately equal to that of water, or with more dense substances. It is obvious that all these features determine the total optical density at each point of the object. In this case, cytoplasmic structures with a low refractive index (for examples, vacuoles filled with liquid) will look like depressions in the phase image of the object, whereas cellular organelles with a high refractive index (nucleus, mitochondria, etc.) will look like protuberances (Fig. 3b). Due to a lower density of the cytoplasm, the phase height at any point of the object will be smaller than that in the part of the cell having the same real height but a low refractive index.

To verify this statement, we compared the neuron images obtained by the methods of optical, laser interference, and confocal microscopy (Fig. 4). It is known that neurons of a pond snail contain plenty of dense granules filled with a carotene pigment [17]. The presence of carotene in granules is illustrated by their absorption spectra (Fig. 5). One can see that more dense regions in the neuron image obtained by optical microscopy (Fig. 4a) correspond to protuberances observed in the LIM image of the neuron (Fig. 4b) and to the fluorescent regions of the cell cytoplasm observed by using confocal microscopy (Fig. 4c). Because intracellular granules have a higher optical density than cytoplasm, the phase image of the neuron is not conical (Fig. 3a) and the total phase height is increased at the edges of the cell (see Fig. 2). Thus, the LIM study of neuron images confirmed the assumption that more dense regions inside the cell correspond to granules containing the pigment.

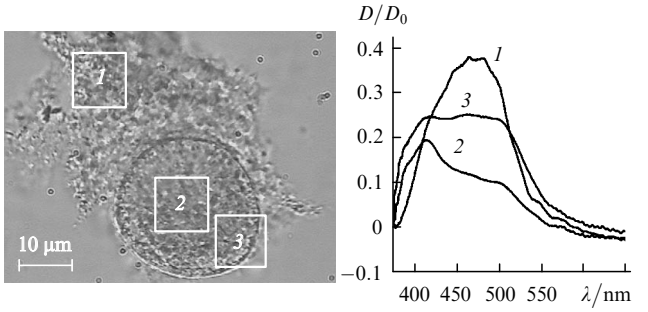

Figure 5. Distribution of cytoplasmic granules containing carotene: (*1*) absorption spectra of carotene in granules outside cells; (*2*) absorption spectra of cytoplasm components; (*3*) absorption spectra of carotene in granules in a cell.

5. Conclusions

Thus, the neuron image obtained by the method of laser interference microscopy has a number of additional characteristics compared to the image obtained by optical microscopy. The volume image of neurons and the distribution of subcellular structures can be obtained and their vertical dimensions can be estimated, which cannot be

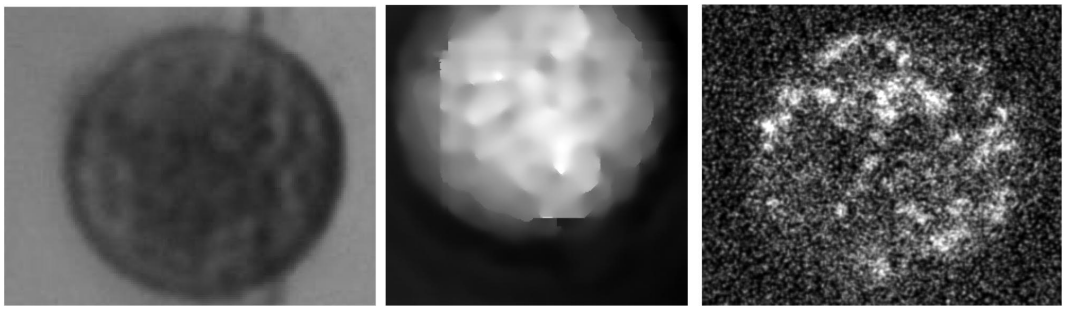

Figure 4. Neuron images obtained by using optical (a), laser interference (b), and confocal (c) microscopy.

achieved by using most of other microscopic methods. In addition, the LIM study of neurons is performed without contrasting the cell image with the help of dyes, i.e. without the violation of the coordinated functioning of the cell. This means that LIM can be used to study variations in the lateral dimensions and volume of cells with the homogeneous cytoplasm and the subcellular relief of the cytoplasm and cellular organelles with the heterogeneous cytoplasm in functioning neurons.

Acknowledgements. The authors thank the Amphora Laboratories LLC for placing a MIM-2.1 microscope at our disposal.

References

1. Brazhe N.A., Erokhova L.A., Churin A.A., Maksimov G.V. *J. Biological Phys.*, **31**, 533 (2005).
2. Erokhova L.A., Novikov S.M., Lazarev G.L., Kazakova T.A., Orlov D.A., Indukaev K.V., Maksimov G.V. *Byul. Eksp. Biol. Med.*, **140**, 237 (2005).
3. Levin G.G., Bulygin F.V., Vishnyakov G.N. *Tsitologiya*, **47**, 348 (2005).
4. Sosnovtseva O.V., Pavlov A.N., Brazhe N.A., Brazhe A.R., Erokhova L.A., Maksimov G.V., Mosekilde E. *Phys. Rev. Lett.*, **94**, 218103 (2005).
5. Tychinsky V.P., Vaiss D., Vyshenskaya T.V., Yaguzhinsky L.S., Nikandrov S.L. *Biofizika*, **45**, 870 (2000).
6. Tychinsky V., Kretushev A., Vyshenskaja T. *Eur. Biophys. J.*, **33**, 700 (2004).
7. Tychinsky V.P., Kretushev A.V., Vyshenskaya T.V., Tikhonov A.N. *Biochim. Biophys. Acta*, **1708**, 362 (2005).
8. Andreev V., Indukaev K. *J. Russ. Laser Res.*, **26**, 380 (2005).
9. Andreev V., Indukaev K., Ioselev O., Legkii A., Lazarev G., Orlov D. *J. Russ. Laser Res.*, **26**, 394 (2005).
10. Maksimov G.V., Nikandrov S.L., Lazareva E.S., Tychinsky V.P., Rubin A.B. *Byul. Eksp. Biol. Med.*, **131**, 539 (2001).
11. Maksimov G.V., Nikandrov S.L., Lazareva E.S., Tychinsky V.P. *Biofizika*, **47**, 345 (2002).
12. Tychinsky V.P., Kretushev A.V., Vyshenskaya T.V., Tikhonov A.N. *Biochim. Biophys. Acta*, **1665**, 57 (2004).
13. Kolomiitsev Yu.V. *Interferomtry* (Interferometers) (Leningrad: Mashinostroenie, 1976).
14. Ukhanov A.A., Tychinskii V.P. *Med. Tekhn.*, **4**, 9 (1996).
15. Andreev V.A., Indukaev K.V. *J. Russ. Laser Res.*, **24**, 220 (2003).
16. Brandon D., Kaplan W.D. *Microstructural Characterization of Materials* (Chichester, West Sussex, UK: John Wiley&Sons LTD, 1999).
17. Erokhova L.A., Brazhe N.A., Maksimov G.V., Rubin A.B. *Dokl. Ross. Akad. Nauk*, **402**, 233 (2005).